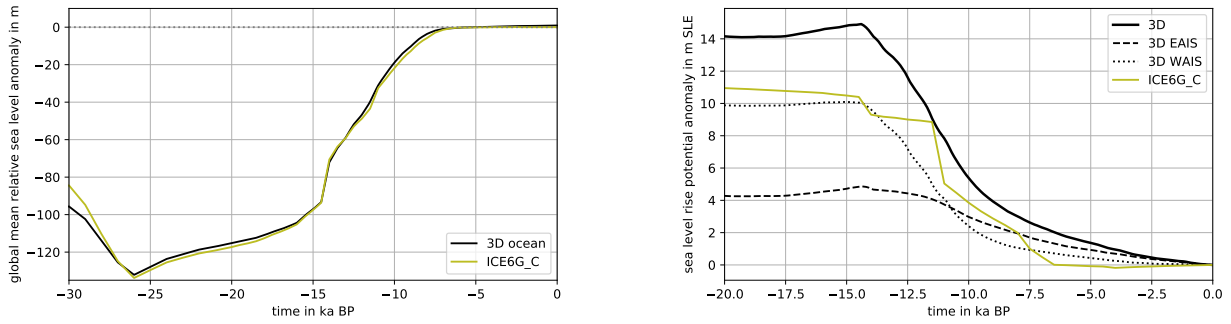


Supplement for manuscript **Oceanic gateways in Antarctica -  
Impact of relative sea-level change on sub-shelf melt**

Moritz Kreuzer, Torsten Albrecht, Lena Nicola, Ronja, Reese, Ricarda Winkelmann

November 17, 2023



**Figure S1. Global mean sea level (left) and Antarctic ice mass (right).** The global Last Glacial Maximum has been reached at ca. 26 ka BP (left), but Antarctica’s LGM was at around 14.5 ka BP. The ICE6G.C dataset (olive color; Stuhne and Peltier, 2015) is included for comparison to the coupled ice sheet-GIA model results from PISM-VILMA (black lines).

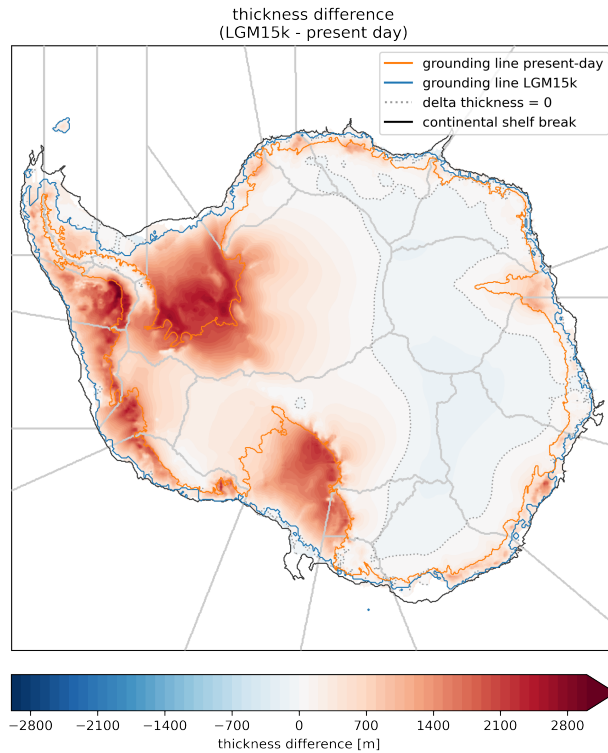


**Figure S2. Ice-sheet thickness difference: LGM15k vs present-day.** Grounding lines are depicted in orange for *present-day* and in blue for *LGM15k* scenario. The continental-shelf break (topography = -1800m) is marked with a black contour line. Change between positive and negative thickness anomaly is highlighted with a dotted grey line.

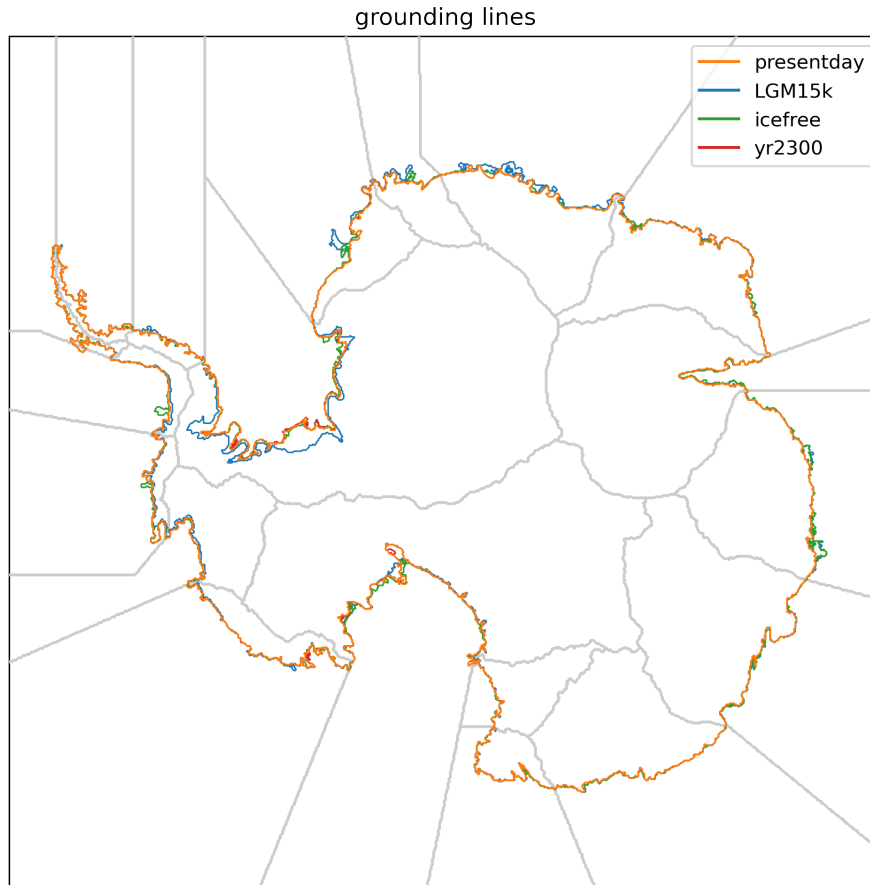


**Figure S3. Horizontally adjusted grounding lines.** After applying vertical bedrock adjustments from relative sea level changes, the grounding line positions have been re-computed via the flotation criterion, using present-day ice-sheet geometry. Basin boundaries are shown in light gray.

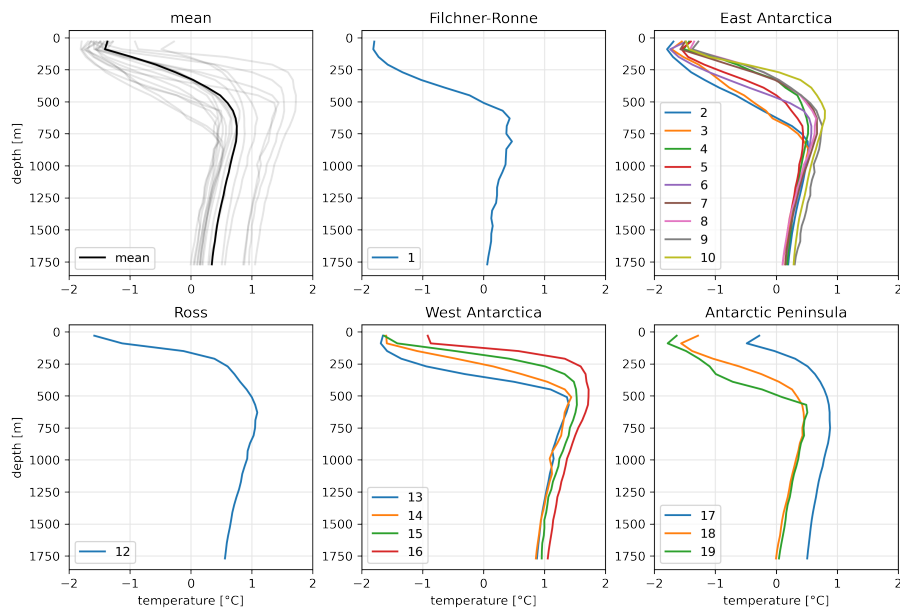


**Figure S4. Vertical temperature profiles at continental-shelf break.** Subplots show horizontal average of vertical potential temperature profiles at all continental-shelf break grid points in each basin. Legends indicate basin numbers. Upper left subplot shows mean of all basin averages. Continental-shelf break is defined at the  $-1800$  m isobar. Data used from Jourdain et al. (2020).

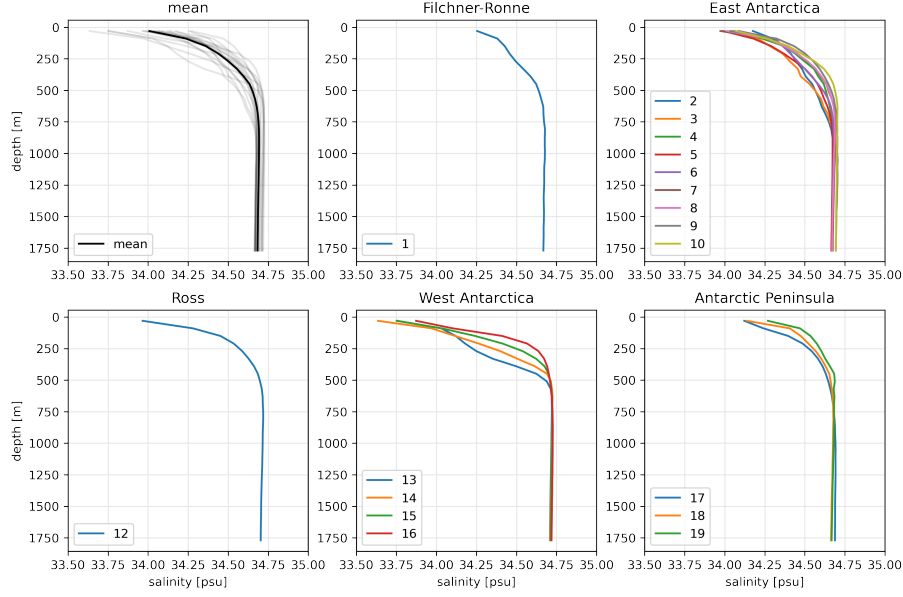


**Figure S5. Vertical salinity profiles at continental-shelf break.** Subplots show horizontal average of vertical practical salinity profiles at all continental-shelf break grid points in each basin. Legends indicate basin numbers. Upper left subplot shows mean of all basin averages. Continental-shelf break is defined at the  $-1800$  m isobar. Data used from Jourdain et al. (2020).

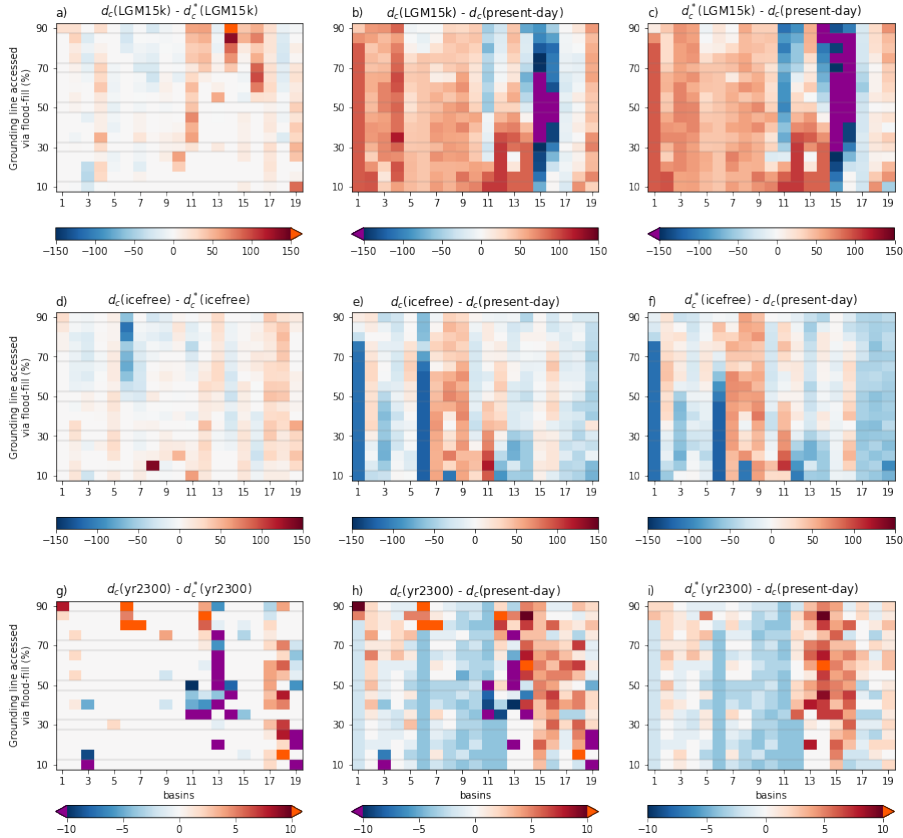


**Figure S6. Comparison of critical access depths with respect to horizontal grounding line adjustment**  $d_c^*$  denotes critical access depths, based on a grounding line position that has not been adjusted to bedrock changes, like used for  $d_c$ . The adjustment leads to a dampening of the critical access depth difference signal in most cases, but also introduces additional noise that can most clearly be seen in the year 2300 scenario. Suppl. Fig. 7 and 8 show changes of  $T_{csb}$ ,  $S_{csb}$  and melt rates based on critical access depth without horizontal grounding line adjustment  $d_c^*$ .

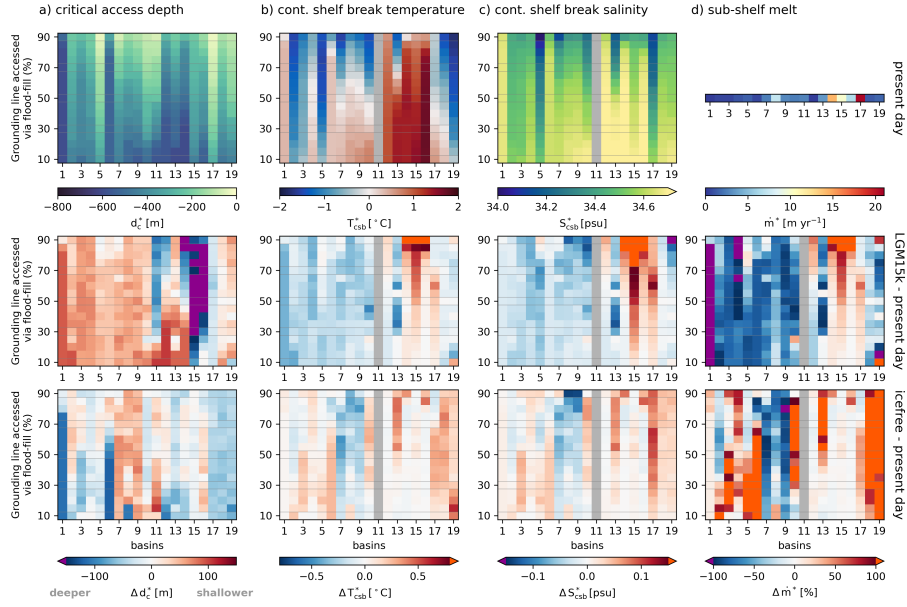


Figure S7. Replication of Fig. 6 without horizontal grounding line adjustment

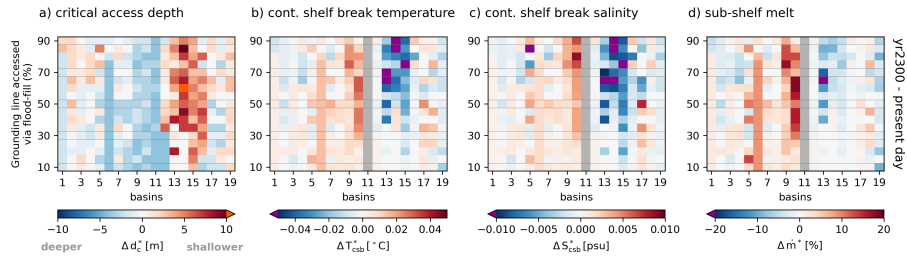


Figure S8. Replication of Fig. 7 without horizontal grounding line adjustment

## References

- Jourdain, N. C., Asay-Davis, X., Hattermann, T., Straneo, F., Seroussi, H., Little, C. M., and Nowicki, S.: A protocol for calculating basal melt rates in the ISMIP6 Antarctic ice sheet projections, *The Cryosphere*, 14, 3111–3134, <https://doi.org/10.5194/tc-14-3111-2020>, 2020.
- Stuhne, G. R. and Peltier, W. R.: Reconciling the ICE-6G\_C reconstruction of glacial chronology with ice sheet dynamics: The cases of Greenland and Antarctica, *Journal of Geophysical Research: Earth Surface*, 120, 1841–1865, <https://doi.org/10.1002/2015jf003580>, 2015.